Dynamic Modeling of the Servovalves Incorporated in the Servo Hydraulic System of the 70-Meter DSN Antennas

R. D. Bartos
Ground Antennas and Facilities Engineering Section

As the pointing accuracy and service life requirements of the DSN 70-meter antennas increase, it is necessary to gain a more complete understanding of the servo hydraulic system in order to improve system designs to meet the new requirements. This article develops a mathematical model for the servovalve incorporated into the hydraulic system of the 70-meter antenna and uses experimental data to verify the validity of the model and to identify the model parameters.

I. Introduction

JPL has long maintained the objective of improving the performance and operating life of the DSN 70-meter antennas. A mathematical model of the servovalve incorporated into the 70-meter antenna servo hydraulic system was created to gain a better understanding of the operation of the hydraulic system as one step toward this objective. During the development of the hydraulic servovalve model several approaches were considered. The first approach consisted of physically modeling the dynamic and steady state operation of each of the internal valve components and combining these models as a system to obtain the servovalve model. The internal valve components include the spool, bushing, feedback wire, flappers, nozzles, and torque motor. Due to the complexity of performing this type of analysis and the inevitable uncertainty of the model due to manufacturing tolerances and complex geometries of internal fluid flow paths, this model was determined to be inappropriate. An alternative model that mathematically describes the performance of the servovalve based upon experimental data was found to predict valve performance with reasonable accuracy. This type of model had its advantages over the physically based model because it was easily implemented within standard simulation packages. Also, the valve manufacturer performs quality assurance tests to insure that the parameters of the experimentally based model are within allowable limits. Because of the stated advantages, the experimentally based model was selected to model the servovalve located within the hydraulic system of the 70-meter antenna.

II. Theoretical Model Development

A. Presentation of Mathematical Equations

Previous experimental investigations have shown that the dynamic response of a flow control servovalve can be approximated by the second-order equations [3,6,7,8]

$$\frac{\partial^2 Q_{c1}}{\partial t^2} = \omega_n^2 \Delta Q_{c1} - 2\xi\omega_n \frac{\partial Q_{c1}}{\partial t} \tag{1}$$

$$\frac{\partial^2 Q_{c2}}{\partial t^2} = \omega_n^2 \Delta Q_{c2} - 2\xi\omega_n \frac{\partial Q_{c2}}{\partial t} \tag{2}$$

where

$$\Delta Q_{c1} = K_v U \sqrt{\frac{2\,|P_S - P_{c1}|}{\rho}}$$

$$\times \operatorname{sgn}(P_S - P_{c1}) - Q_{c1} \quad U \geq 0 \tag{3}$$

$$\Delta Q_{c1} = K_v U \sqrt{\frac{2\,|P_{c1} - P_T|}{\rho}}$$

$$\times \operatorname{sgn}(P_{c1} - P_T) - Q_{c1} \quad U < 0 \tag{4}$$

$$\Delta Q_{c2} = -K_v U \sqrt{\frac{2\,|P_{c2} - P_T|}{\rho}}$$

$$\times \operatorname{sgn}(P_{c2} - P_T) - Q_{c2} \quad U \geq 0 \tag{5}$$

$$\Delta Q_{c2} = -K_v U \sqrt{\frac{2\,|P_S - P_{c2}|}{\rho}}$$

$$\times \operatorname{sgn}(P_S - P_{c2}) - Q_{c2} \quad U < 0 \tag{6}$$

$$U = i - i_{NB} + i_T + i_H + i_X$$

$$|i - i_{NB} + i_T + i_H + i_X| \leq i_{SAT} \tag{7}$$

$$U = i_{SAT} \operatorname{sgn}(i - i_{NB} + i_T + i_H + i_X)$$

$$|i - i_{NB} + i_T + i_H + i_X| > i_{SAT} \tag{8}$$

$$K_v = K_1 \quad |i - i_{NB} + i_T + i_H| \leq i_{cr} \tag{9}$$

$$K_v = K_2 \quad |i - i_{NB} + i_T + i_H| > i_{cr} \tag{10}$$

$$i_X = 0 \quad |i - i_{NB} + i_T + i_H| \leq i_{cr} \tag{11}$$

$$i_X = i_X^* \operatorname{sgn}(i - i_{NB} + i_T + i_H)$$

$$|i - i_{NB} + i_T + i_H| > i_{cr} \tag{12}$$

The above variables, to be described in greater detail later in this article, are defined as

i = input current to the valve

i_{cr} = critical current defining the boundary of the null flow region

i_H = servovalve hysteresis current

i_{NB} = servovalve null bias current

i_{SAT} = lowest current input at which the flow limit of the valve is reached

i_T = compensating current to model threshold

i_X = X-axis intercept current adjustment

i_X^* = X-axis intercept current relative to null

K_v = valve proportionality constant

i_X^* = X-axis intercept current relative to null

K_v = valve proportionality constant

K_1 = valve proportionality constant near null

K_2 = valve proportionality constant away from null

P_{c1} = pressure at control port no. 1

P_{c2} = pressure at control port no. 2

P_S = supply pressure

P_T = tank or return pressure

Q_{c1} = flow rate out of control port no. 1

Q_{c2} = flow rate out of control port no. 2

t = time

U = effective command signal

ρ = fluid density

ω_n = valve natural frequency

ξ = damping ratio

B. Pressure-Drop-to-Flow Relationship

A servovalve operates by metering fluid flow from the supply line to one control port and from the other control port to the return line by using a restriction with a pressure-drop-to-flow relationship equivalent to that of an orifice. Using the orifice model, the fluid flow rate from the supply line to the control ports and from the control ports to the return line varies with the square root of the pressure difference across the valve and as the square root of

the inverse of the fluid density. Equations (3) through (6) provide a mathematical description of the orifice behavior.

C. Flow Gain

Servovalves are manufactured to produce a linear flow gain with respect to input current for a given valve pressure drop. In practice the flow gain is modeled as a piecewise linear function. There are three linear regions of the flow curve as shown in Fig. 1. The three regions are referred to as the null region, the normal flow region, and the flow saturation region. Within the null region where the current input to the valve is $\pm i_{cr}$ of the null position, the valve exhibits a linear flow gain K_1 according to Eq. (9). The value of the flow gain K_1 is dependent upon the lap of the valve. Critically lapped valves exhibit a flow gain that is equivalent to the flow gain K_2 found in the region of normal flow while valves that are overlapped and underlapped have flow gains that are lower and higher than K_2, respectively. The region of normal flow is the designed operating range of the valve where the rated flow gain K_2 occurs. Once the current input to the valve exceeds a certain level, flow saturation occurs. When saturation exists the flow gain decreases in a nonlinear fashion until the flow limit of the valve is reached. At the flow limit of the valve an increase in current input to the valve results in no increase of flow to the control port. The behavior of the flow gain in the flow saturation region is governed by such things as the stability of the supply pressure at high valve flow rates and the mechanical limitations placed on the valve spool. Since the supply pressure to the servovalve is fairly constant on the 70-meter antenna, the region of saturation is modeled as an abrupt change from the region of normal flow to the valve flow limit.

D. Null Bias

The null bias of a valve is the input current required to bring the valve to its null position under a certain set of operating conditions not including the effects of hysteresis. The null bias of the valve is modeled in Eq. (7) by the variable i_{NB}.

E. Threshold

Threshold is the increment of current input required to produce a change in valve flow rate when changing the direction of the applied current to the valve. A valve flow curve illustrating threshold is shown in Fig. 2. Threshold is mathematically modeled in Eq. (7) by the variable i_T and is computed once every sampling period that a current signal is sent to the servovalve by the following logic statements:

If $i > i_k + \varepsilon$ then (13)

$F_{k+1} = 1$ (14)

$i_{k+1} = i$ (15)

else if $i < i_k - \varepsilon$ then (16)

$F_{k+1} = -1$ (17)

$i_{k+1} = i$ (18)

else

$F_{k+1} = F_k$ (19)

$i_{k+1} = i_k$ (20)

end if

If $F_{k+1} \times F_k = -1$ then (21)

if $i_k > i_A$ then (22)

$i_A = i_k$ (23)

$i_B = i_A - i_T^*$ (24)

else if $i_k < i_B$ then (25)

$i_B = i_k$ (26)

$i_A = i_B + i_T^*$ (27)

end if

end if

If $i > i_A$ then (28)

$i_T = -\frac{1}{2} i_T^*$ (29)

else if $i < i_B$ then (30)

$i_T = \frac{1}{2} i_T^*$ (31)

else

$i_T = i_A - i - \frac{1}{2} i_T^*$ (32)

end if

$k = k + 1$ (33)

where

F_k = logical variable that indicates the direction of application of the input current. The variable takes on the values of -1 for decreasing current and $+1$ for increasing current.

i = input current to the valve

i_A = upper endpoint of current range where flow does not change

i_B = lower endpoint of current range where flow does not change

i_k = input current to the valve at sample interval k

i_T = input current adjustment required to model threshold

i_T^* = threshold current

k = sample interval

ε = amplitude of input current signal noise

Equations (13) through (20) are designed to keep track of whether the input current is increasing or decreasing while taking into consideration the amplitude of the input signal noise. A change in the direction of current application is detected by Eq. (21), while Eqs. (22) through (27) are used to redefine the current region where invariant flow occurs, as shown in Fig. 3. The adjustment to the input current required to model the threshold phenomenon is computed using Eqs. (28) through (32). Equation (33) is used to increment the sampling interval index. The logical statements used to model threshold have been restated in flow diagram format in Fig. 4.

F. Hysteresis

During a single cycle of the input signal, a given flow rate is achieved twice: once as the signal increases and once as it decreases. Hysteresis is the difference in valve current inputs required to produce this flow rate. The magnitude of hysteresis increases with the amplitude at which the input signal is cycled, as shown in Fig. 5. When the current is cycled at low amplitudes, the hysteresis effects are contained within the threshold model. As the amplitude of the current cycle is increased, additional modeling is required to predict valve performance. During the operation of the hydraulic system of the 70-meter antenna, the servovalve will operate closely around a single input current as opposed to cycling through its full operating range. Under these conditions the threshold model is sufficient to describe the hysteresis effects of the valve. Because the slewing of the antenna operates over the full region of the valve, the flow curve of the valve may shift within the limits of the valve hysteresis depending upon the current signal history prior to antenna tracking. The shift of the flow gain curve due to hysteresis is modeled by the variable i_H in Eq. (7). The variable i_H is treated as a statistical variable that changes over extended periods of time and takes on values within a specific distribution.

III. Experimental Investigation

A. Overview

During the investigation of the performance characteristics of the Moog 72-163B servovalve at JPL, experimental programs were undertaken both at Moog under the direction of Peter Hames and at Fluid Technologies, Inc., under the direction of Elizabeth Carrell. The results gathered during these investigations were used to identify the parameters of the theoretical model presented in the previous section and to estimate the accuracy of the model.

B. Frequency Response

The frequency response characteristics of the Moog 72-163B servovalve were determined through experiments conducted at Moog on January 27, 1988. It was concluded from an analysis of the results that the dynamic response of the servovalve is best approximated by a second-order model with a natural frequency of 55 hertz and a damping ratio of 0.8. Both the experimental frequency response and the second-order model approximations are presented in Figs. 6 and 7.

C. Hysteresis and Threshold

The hysteresis and threshold effects of the Moog 72-163B servovalve no. 110 were experimentally determined at Moog on April 19, 1988. The experimental results indicated a hysteresis of 0.1 milliampere when the valve was cycled between negative and positive full flow. A threshold current of 0.01 milliampere was also observed during the testing of the valve.

D. Steady State Flow Characteristics

An experimental program was conducted at Fluid Technologies, Inc., to determine the effect that the geometrical dimensions of the valve spool have upon servovalve flow characteristics. The program was conducted between December 31, 1990, and January 7, 1991. The spool dimensions along with the supply pressures for each of the experiments are shown in Fig. 8. Details of the experimental hardware and procedures are presented in [1,2,4,5].

E. Data Reduction

The valve flow constant K_v and the X-axis intercept of the flow curve were computed by performing a least squares fit of the experimental flow rate versus input current data using the computer program MATLAB. The data points contained in the negative, null, and positive flow regions of the servovalve were fit to a first-order polynomial separately in order to conform to the piecewise linear theoretical model. Some of the data points obtained at the higher current input magnitudes were removed prior to fitting the model to the data. The removal of the data points believed to be invalid was done because the valve was observed to saturate at flow rates near the maximum output capability of the pump supplying fluid to the servovalve. Therefore, it was suspected that the supply pres-

output capability of the pump supplying fluid to the servovalve. Therefore, it was suspected that the supply pressure to the valve was not constant at the larger input current magnitudes. There was no way of knowing whether the supply pressure was actually constant since the supply pressure was not monitored continuously during the experiments. Hence, some data points were removed where saturation of the valve was observed. The parameters that were identified from the least squares fit of the data are presented in Table 1, while a plot of both the experimental and theoretical valve flow curves are shown by the example in Fig. 9. It is evident from an examination of Fig. 9 that the experimental flow curves of the positive and negative flow regions did not necessarily match the flow curve of the null region from a continuity standpoint. This lack of continuity occurs because the data taken in the null region were obtained in a separate experimental run from the data taken in the normal flow region. Hence, the observed discontinuity is attributed to the effects of hysteresis and threshold. For this reason, the data taken in the null region were used only to identify the valve flow constant. The results presented in Table 1 indicate that the valve-flow-gain constant, K_v, is slightly different for the positive and negative flow regions contrary to expectation. This small difference is believed to be the result of the valve spool and bushing not being "exactly" symmetrical about null. When modeling the valve in computer simulation programs, an average of the valve flow constant in the positive and negative flow regions should be used to model the valve in the region of normal flow. The null bias of the valve was taken to be the midpoint of where the positive and negative flow curves intersect the X-axis. The value of the X-axis intercept current, i_X^*, used in the servovalve model is taken to be one half the current magnitude between the locations where the positive and negative flow curves intersect the X-axis. The current value for the variable i_{cr} that defines the boundary of the null flow region is computed by finding the current at which the linear flow curve of the null region intersects the linear flow curve of the normal flow region. The servovalve model parameters for each of the experimental valves is presented in Table 2.

F. Summary of Results

Experimental methods were implemented to determine the parameters for the Moog 72-163B servovalve according to the servovalve model presented in Section II. The model parameter values that should be used when simulating the valve in the hydraulic system of the 70-meter antenna are presented in Tables 2 and 3.

IV. Conclusion

In order to more completely understand the dynamic behavior of the servo hydraulic system of the 70-meter antennas located in the DSN, a mathematical model for a servovalve was developed. Experimental data were used to identify the model parameters for the Moog 72-163B servovalves that are incorporated into the hydraulic system of the 70-meter antenna. The servovalve performance predicted by the theoretical servovalve model was found to be in excellent agreement with the experimental data.

Acknowledgments

The author thanks Fredrick J. Menninger and Ben A. Parvin for their support during the experimental program.

References

[1] E.-A. Carrell, "Investigation of Mechanical Wear Effects on Servovalve Performance," Master of Science thesis, Massachusetts Institute of Technology, Cambridge, Massachusetts, June 1991.

[2] A. Khalil, *Servovalve Performance Assessment—Final Report*, Report no. VT90108, Fluid Technologies, Inc., Stillwater, Oklahoma, March 1991.

[3] H. E. Merritt, *Hydraulic Control Systems*, New York: John Wiley & Sons, 1967.

[4] *Catalog 72-890A*, Moog Inc., East Aurora, New York.

[5] *Electrohydraulic Servovalve 72 Series Service Manual*, Moog Inc., East Aurora, New York, 1990.

[6] W. J. Thayer, *Specifications Standards for Electrohydraulic Flow Control Servovalves*, Technical Bulletin 117, Moog Inc., East Aurora, New York, 1962.

[7] W. J. Thayer, *Transfer Functions For Moog Servovalves*, Technical Bulletin 103, Moog Inc., East Aurora, New York, 1962.

[8] J. Watton, *Fluid Power Systems Modeling, Simulation, Analog, and Microcomputer Control*, New York: Prentice Hall, 1989.

Table 1. Servovalve parameters.

Valve ID	Negative flow region			Null flow region			Positive flow region		
	K_v, m^2/mA	I_x, mA	σ^2, $(m^3/sec)^2$	K_v, m^2/mA	I_x, mA	σ^2, $(m^3/sec)^2$	K_v, m^2/mA	I_x, mA	σ^2, $(m^3/sec)^2$
A-1	1.08E−06	−5.43E−01	1.89E−10	3.90E−07	−3.94E−01	8.30E−10	1.18E−06	3.01E−01	1.40E−10
A-2	1.05E−06	−3.73E−01	2.45E−10	2.83E−06	2.43E−01	6.81E−10	1.13E−06	6.77E−01	6.86E−11
A-3	1.08E−06	−1.46E−01	2.53E−10	1.99E−06	5.85E−01	5.63E−10	1.07E−06	8.87E−01	1.03E−09
A-4	9.99E−07	−6.17E−01	5.40E−11	1.03E−06	8.86E−02	1.71E−09	1.04E−06	5.29E−01	8.30E−11
B-1	1.15E−06	−1.42E+00	4.51E−11	7.90E−08	−8.68E−01	5.60E−12	1.20E−06	2.80E−01	1.96E−10
B-2	1.06E−06	−4.53E−01	7.88E−11	3.38E−07	−1.32E−01	2.73E−11	1.11E−06	5.74E−01	1.06E−10
B-3	1.17E−06	−4.29E−01	7.52E−11	1.45E−07	3.28E−02	3.12E−12	1.23E−06	4.36E−01	5.55E−11
B-4	1.02E−06	−3.16E−01	8.06E−11	8.72E−07	4.21E−02	2.52E−10	1.05E−06	2.18E−01	9.37E−11
B-5	1.13E−06	−3.22E−01	1.57E−10	1.01E−06	−3.63E−03	1.80E−10	1.17E−06	1.15E−01	1.43E−10
C-1	1.05E−06	−6.60E−01	5.35E−11	3.27E−07	−2.10E−01	9.29E−11	1.15E−06	4.32E−01	7.28E−11
C-2	1.17E−06	−8.48E−01	1.60E−10	5.11E−07	−6.99E−01	2.27E−11	1.26E−06	−2.07E−01	6.94E−11
C-3	1.04E−06	−7.54E−01	8.08E−11	1.13E−07	−8.64E−02	5.00E−12	1.10E−06	6.58E−01	1.34E−10
C-4	1.02E−06	−7.96E−01	4.36E−11	3.00E−09	3.24E−01	5.00E−13	1.06E−06	1.15E+00	1.46E−10
D-1	1.46E−06	7.02E−03	4.41E−10	1.08E−06	4.12E−02	4.91E−11	1.53E−06	3.10E−01	2.76E−10
D-2	1.23E−06	−5.14E−01	1.95E−10	1.14E−06	3.02E−01	1.32E−10	1.38E−06	6.73E−01	9.01E−10

K_v = valve proportionality constant.
I_x = X-axis intercept.
σ^2 = variance of the residuals.

Table 2. Servovalve model parameters.

Valve ID	K_1, m^2/mA	K_2, m^2/mA	i_X^*, mA	i_{cr}, mA	i_{NB}, mA
A-1	3.89E−07	1.13E−07	4.22E−01	6.45E−01	−1.22E−01
A-2	2.83E−06	1.09E−06	5.25E−01	−3.27E−01	1.52E−01
A-3	1.99E−06	1.07E−06	5.17E−01	−6.08E−01	3.71E−01
A-4	1.03E−06	1.02E−06	5.73E−01	−6.85E+01	−4.39E−02
B-1	7.91E−08	1.18E−06	8.52E−01	9.13E−01	−5.71E−01
B-2	3.38E−07	1.09E−06	5.14E−01	7.45E−01	6.04E−02
B-3	1.45E−07	1.20E−06	4.32E−01	4.92E−01	3.08E−03
B-4	8.72E−07	1.04E−06	2.67E−01	1.69E+00	−4.89E−02
B-5	1.01E−06	1.15E−06	2.19E−01	1.80E+00	−1.04E−01
C-1	3.27E−07	1.10E−06	5.46E−01	7.76E−01	−1.14E−01
C-2	5.11E−07	1.22E−06	3.21E−01	5.53E−01	−5.27E−01
C-3	1.13E−07	1.07E−06	7.06E−01	7.89E−01	−4.80E−02
C-4	2.85E−09	1.04E−06	9.72E−01	9.75E−01	1.77E−01
D-1	1.08E−06	1.49E−06	1.51E−01	5.48E−01	1.58E−01
D-2	1.14E−06	1.31E−06	5.93E−01	4.65E+00	7.96E−02

K_1 = valve proportionality constant in the null flow region.
K_2 = valve proportionality constant in the normal flow region.
i_x^* = X-axis intercept relative to null.
i_{cr} = critical current defining the null flow region.
i_{NB} = null bias.

Table 3. Servovalve model parameters.

Parameter	Value
i_H, mA	±0.1
i_{SAT}, mA	20 (rated current)
i_T^*, mA	0.01
P_S, bar	172.4
P_T, psi	0
ρ, kg/m^3	854
ω_n, Hz	55
ξ	0.8

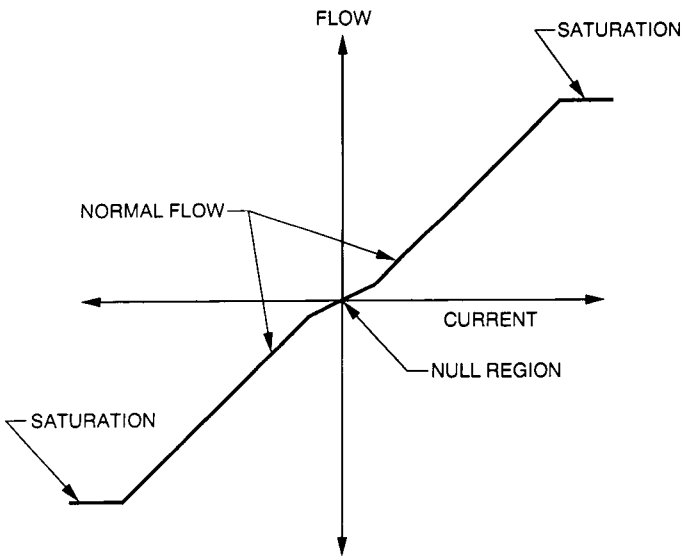

Fig. 1. Servovalve flow curve at a constant pressure drop.

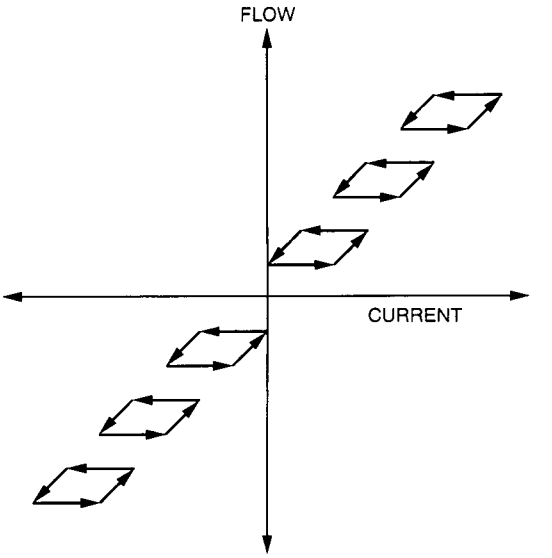

Fig. 2. Threshold loops.

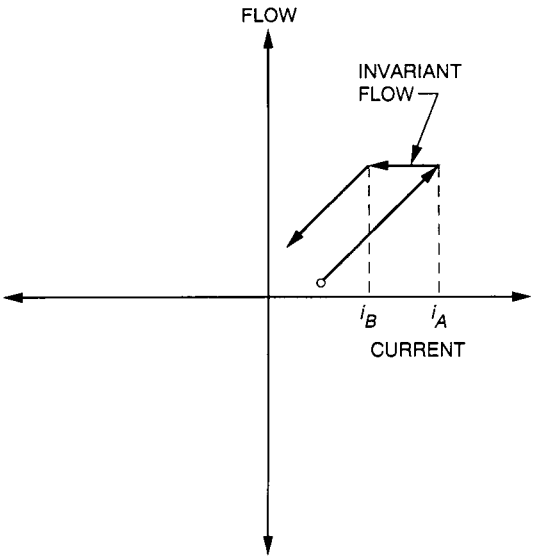

Fig. 3. Invariant flow region.

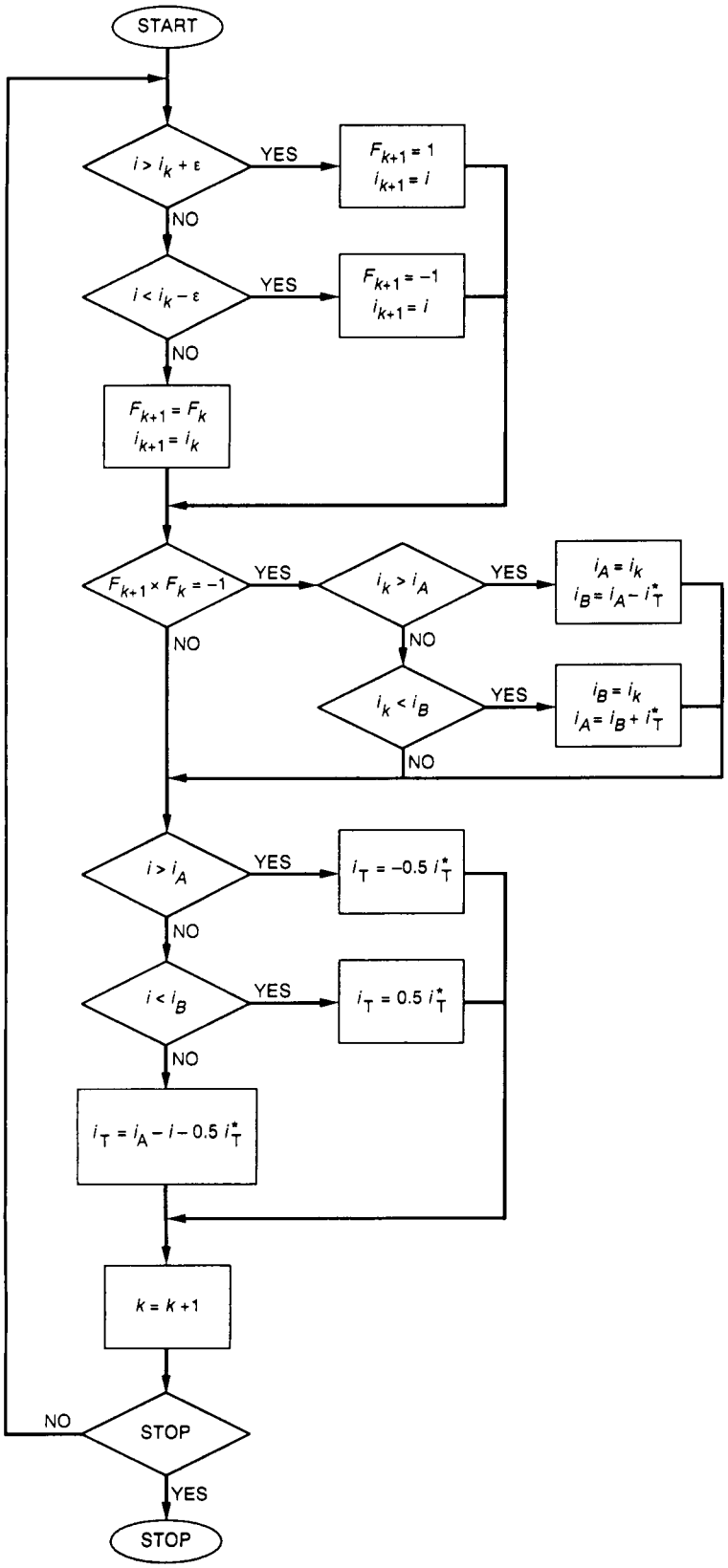

Fig. 4. Threshold model.

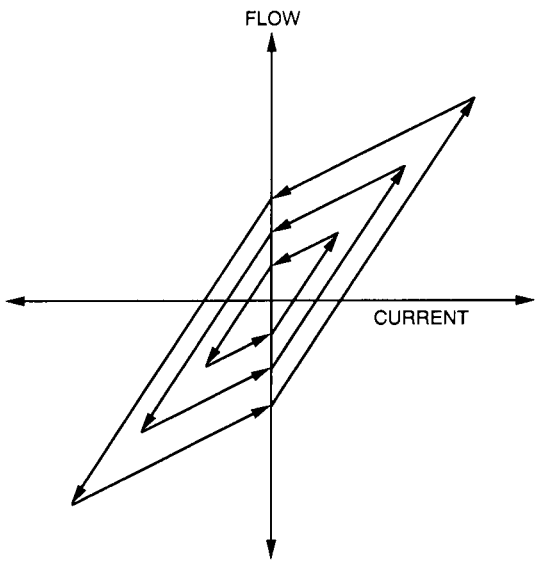

Fig. 5. Servovalve hysteresis.

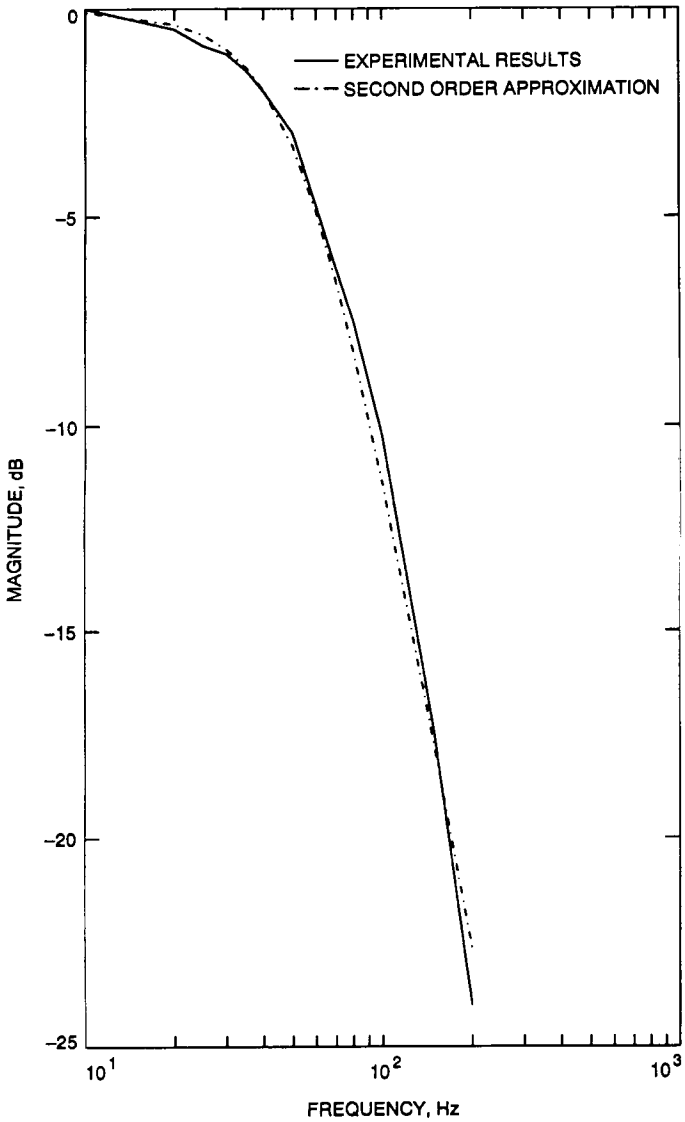

Fig. 6. Magnitude frequency response of Moog 72-163B servovalve; supply pressure = 172.4 bar.

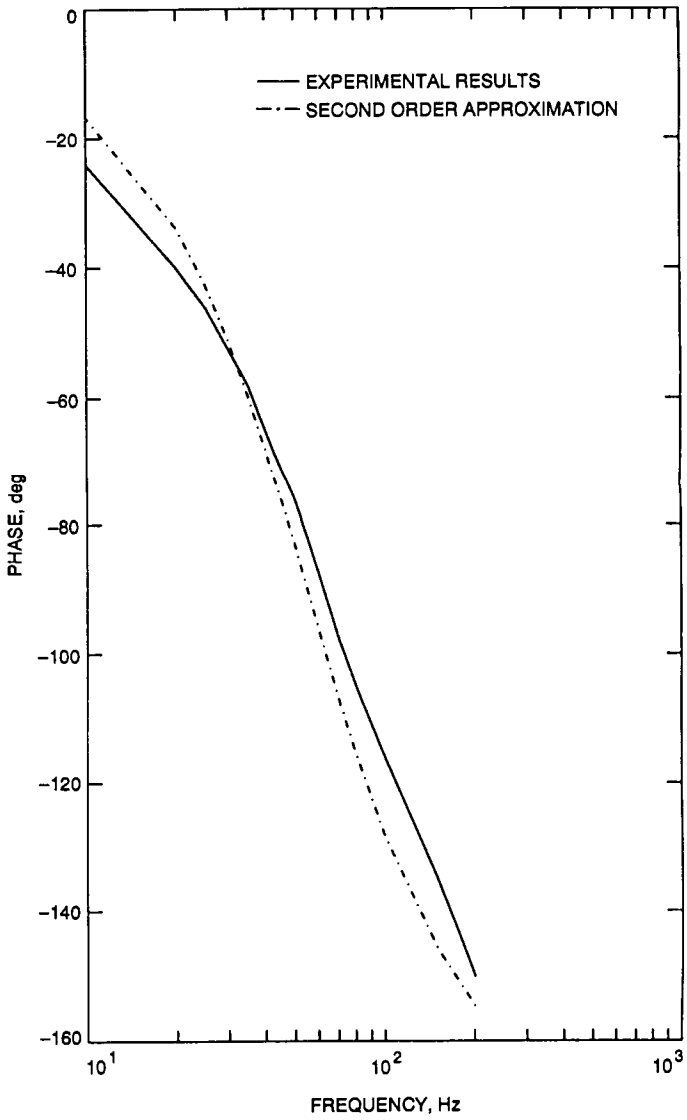

Fig. 7. Phase angle frequency response of Moog 72-163B servovalve; supply pressure = 172.4 bar.

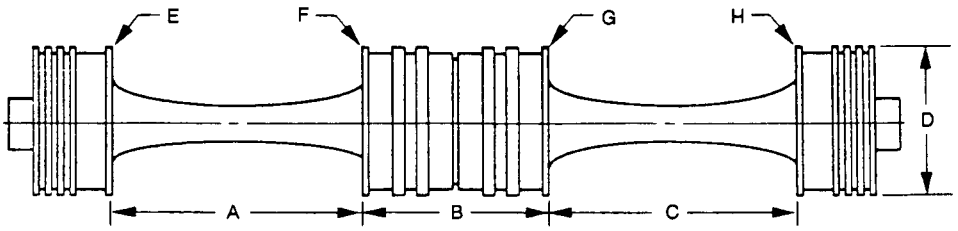

VALVE ID	SPOOL DIMENSIONS								PRESSURE (PSI)
	A (in.)	B (in.)	C (in.)	D (in.)	E (mm)	F (mm)	G (mm)	H (mm)	
A-1	0.999	1.003	1.001	0.74975	0.03	0.03	0.03	0.03	2500
A-2	"	"	"	"	0.08	0.09	0.09	0.09	2500
A-3	"	"	"	"	0.15	0.17	0.16	0.15	2500
A-4	"	"	"	"	0.32	0.35	0.34	0.33	2500
B-1	0.993	1.005	0.9965	0.7498	0.05	0.01	0.04	0.03	2500
B-2	0.9963	1.0017	0.9986	"	0.04	0.02	0.03	0.02	2500
B-3	REPEAT OF VALVE B-2								1800
B-4	1	0.9976	0.9975	"	0.03	0.03	0.02	0.02	2500
B-5	REPEAT OF VALVE B-4								1800
C-1	1.0005	0.9975	0.9995	0.7499	0.03	0.02	0.04	0.04	2500
C-2	REPEAT OF VALVE C-1								1800
C-3	"	"	"	0.7495	0.02	0.02	0.03	0.03	2500
C-4	"	"	"	0.7491	0.01	0.01	0.01	0.01	2500
C-5	REPEAT OF VALVE C-4								1800
D-1	0.9975	0.997	0.998	0.7499	0.05	0.05	0.06	0.14	2500
D-2	0.005 AXIAL SCRATCH EQUALLY SPACED THREE PLACES								2500
D-3	0.010 AXIAL SCRATCH EQUALLY SPACED THREE PLACES								2500

Fig. 8. Servovalve spool dimensions and locations.

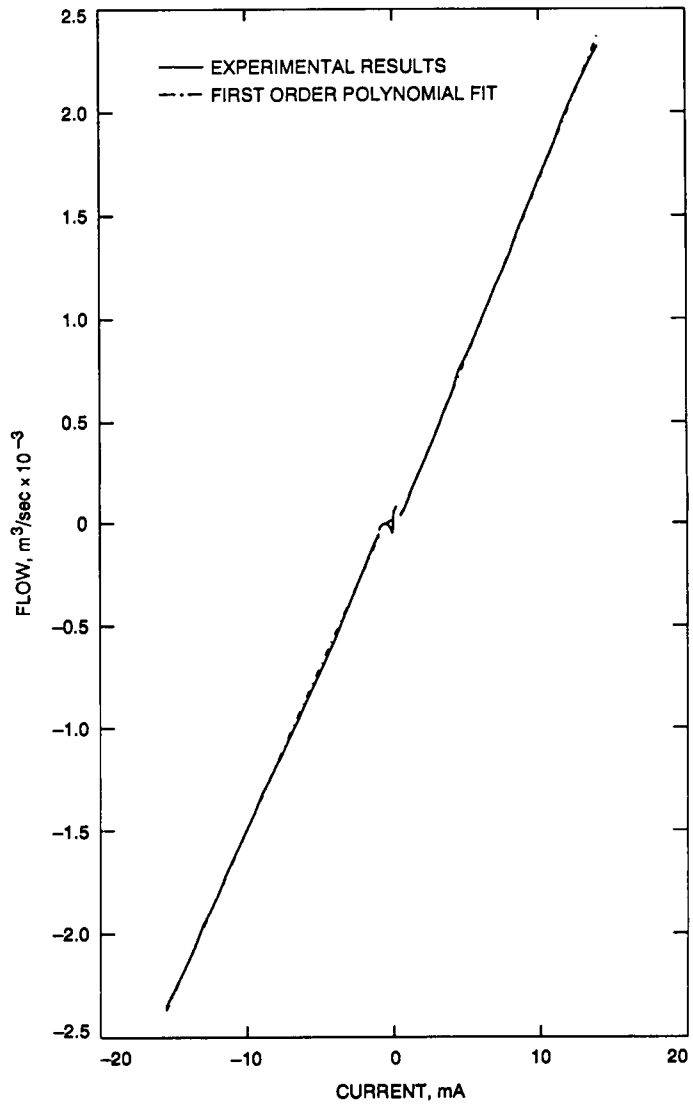

Fig. 9. Flow gain curve of servovalve B-3; supply pressure = 124.1 bar.